AUTOPHAGY
2016, VOL. 12, NO. 12, 2271–2285
http://dx.doi.org/10.1080/15548627.2016.1230583

Taylor & Francis
Taylor & Francis Group

BASIC RESEARCH PAPER

Thyroid hormone suppresses hepatocarcinogenesis via DAPK2 and SQSTM1-dependent selective autophagy

Hsiang-Cheng Chi[a], Shen-Liang Chen[b], Chung-Ying Tsai[a], Wen-Yu Chuang[c], Ya-Hui Huang[d], Ming-Ming Tsai[e,f], Sheng-Ming Wu[a,g], Cheng-Pu Sun[h], Chau-Ting Yeh[d], and Kwang-Huei Lin[a,d]

[a]Department of Biochemistry, College of Medicine, Chang-Gung University, Taoyuan, Taiwan; [b]Department of Life Sciences, National Central University, Jhongli, Taiwan; [c]Department of Pathology, Chang Gung Memorial Hospital and Chang Gung University College of Medicine, Taoyuan, Taiwan; [d]Liver Research Center, Chang Gung Memorial Hospital, Linkou, Taoyuan, Taiwan; [e]Department of Nursing, Chang-Gung University of Science and Technology, Taoyuan, Taiwan; [f]Department of General Surgery, Chang Gung Memorial Hospital at Chiayi, Taiwan; [g]Division of Pulmonary Medicine, Department of Internal Medicine, Shuang Ho Hospital, Taipei Medical University; [h]Institute of Biomedical Sciences, Academia Sinica, Taipei, Taiwan

ABSTRACT

Recent studies have demonstrated a critical association between disruption of cellular thyroid hormone (TH) signaling and the incidence of hepatocellular carcinoma (HCC), but the underlying mechanisms remain largely elusive. Here, we showed that disruption of TH production results in a marked increase in progression of diethylnitrosamine (DEN)-induced HCC in a murine model, and conversely, TH administration suppresses the carcinogenic process via activation of autophagy. Inhibition of autophagy via treatment with chloroquine (CQ) or knockdown of ATG7 (autophagy-related 7) via adeno-associated virus (AAV) vectors, suppressed the protective effects of TH against DEN-induced hepatic damage and development of HCC. The involvement of autophagy in TH-mediated protection was further supported by data showing transcriptional activation of DAPK2 (death-associated protein kinase 2; a serine/threonine protein kinase), which enhanced the phosphorylation of SQSTM1/p62 (sequestosome 1) to promote selective autophagic clearance of protein aggregates. Ectopic expression of DAPK2 further attenuated DEN-induced hepatoxicity and DNA damage though enhanced autophagy, whereas, knockdown of DAPK2 displayed the opposite effect. The pathological significance of the TH-mediated hepatoprotective effect by DAPK2 was confirmed by the concomitant decrease in the expression of THRs and DAPK2 in matched HCC tumor tissues. Taken together, these findings indicate that TH promotes selective autophagy via induction of DAPK2-SQSTM1 cascade, which in turn protects hepatocytes from DEN-induced hepatotoxicity or carcinogenesis.

ARTICLE HISTORY
Received 16 September 2015
Revised 12 August 2016
Accepted 25 August 2016

KEYWORDS
DAPK2; HCC; selective autophagy; SQSTM1/p62; THR

Introduction

The active form of thyroid hormone (TH), 3, 3′5-triiodo-l-thyronine (T_3), is a potent regulator of cellular and tissue metabolism throughout the body. T_3 activity is mediated through binding to its cognate thyroid hormone receptors (THRA and THRB). In the absence of ligands, THRs bind to the T_3 response elements (TREs) of target genes and suppress their expression. Binding of T_3 transforms THRs into activators that stimulate expression of these genes.[1]

Liver is a critical target organ of TH, and imbalance in TH-THRs signals is known to underlie hepatic diseases, such as chronic hepatitis and HCC.[1] For instance, v-erbA, a mutant form of THRA lacking ligand binding ability, is reported to cause HCC in transgenic mice.[2] A recent epidemiological study suggests that long-term hypothyroidism is positively correlated with HCC incidence, independent of other risk factors.[3] These studies indicate that the T_3-THRs pathway not only mediates hepatic homeostasis but also serves as a tumor repressor in liver. Analysis of the genes/signals downstream of T_3 in hepatocytes should therefore shed light on the mechanisms underlying the antagonistic effects of the T_3-THRs pathway against HCC progression.

Autophagy is a self-digestion process involving the capture, recycling or degradation of impaired components or aggregated proteins in lysosomes to maintain organelle quality and cellular homeostasis.[4] The roles of autophagy in hepatic homeostasis have been increasingly explored in recent years. Disruption of autophagic flux impairs the energy metabolism balance for cellular functions in liver, which causes a major impact on hepatic physiology and disease.[5] Additionally, mosaic deletion of the essential autophagy genes, *Atg5* (autophagy-related 5) or liver-specific *Atg7*, in mice, leads to spontaneous HCC development.[6] These studies clearly indicate that normal autophagic flux is important to prevent HCC incidence. Stimulation of this process may therefore present a novel approach in the management of HCC prevention and therapy. DAPK2 is an enzyme belongs to the DAPK family of Ca^{2+}-CALM1 (calmodulin 1)–dependent Ser/Thr kinases.[7] DAPK2 exerts its kinase activity to

CONTACT Kwang-Huei Lin khlin@mail.cgu.edu.tw Department of Biochemistry, Chang-Gung University, 259 Wen-hwa 1 Road, Taoyuan, Taiwan, Republic of China.
Supplemental data for this article can be accessed on the publisher's website.

induce apoptosis in various cell lines. Conversely, suppression of DAPK2 expression rescues cell death triggered by various stimuli, such as TNF (tumor necrosis factor) and IFNG (interferon gamma).[7,8] Recent studies have reported another novel function of DAPK2 during autophagy. Expression of DAPK2 promotes phosphorylation of RPTOR (regulatory associated protein of MTOR, complex 1), and subsequently modulates MTORC1 (mechanistic target of rapamycin [serine/threonine kinase] complex 1) activity and autophagy levels under stress conditions.[9] Gene expression profiling studies reveal that *DAPK2* expression is increased during myeloid differentiation, and DAPK2 enhances all-trans retinoic acid (ATRA)-induced neutrophil maturation, possibly through autophagy rather than apoptosis.[10] Thus, the kinase activity of DAPK2 appears critical in the autophagy-mediated maintenance of cellular homeostasis and survival.

Recent studies have shown that T_3 acts as an autophagy inducer to modulate lipid metabolism.[11,12] However, the mechanism by which autophagy is triggered by T_3 and its involvement in tumor suppression have not been explored to date. Our experiments showed that T_3-THRs signaling induces *DAPK2* expression at the transcriptional level, and its upregulation mediates the T_3-triggered autophagic response, in turn, attenuating DEN-induced hepatotoxicity or hepatocarcinogenesis.

Notably, increasing evidence has demonstrated that selective autophagy is mediated through autophagy receptor proteins, such as SQSTM1, linking autophagy cargos and autophagosomes.[13] Here, we report that DAPK2 induced SQSTM1 phosphorylation to regulate autophagic clearance of ubiquitinated aggregates. Additionally, the expression of DAPK2 was negatively correlated with that of SQSTM1 in HCC specimens. Thus, this study has revealed a mechanistic link between the decreased T_3-THRs pathway and DAPK2 in HCC, providing novel insights into the physiological significance of DAPK2 in prevention of HCC.

Results

Thyroid hormone inhibits DEN-induced hepatic toxicity, DNA damage, inflammation, and hepatocellular carcinogenesis in mice

To establish the roles of T_3 in HCC initiation and progression, euthyroid, hyperthyroid, and hypothyroid mice were treated with DEN (Fig. 1A). DEN has been shown to trigger multiple HCC-like liver tumors in mice.[14] After the addition of DEN to drinking water, hepatic surface tumor nodules were detected at 17 wk in hypothyroid mice and 26 wk in euthyroid mice. In contrast, very few or no HCC nodules were observed in mice receiving T_3 treatment, even at 26 wk after DEN administration (Fig. 1B, C). Histological sections of livers from these groups of mice at various treatment time-points revealed that hepatocarcinoma development is accelerated under hypothyroid status (Fig. 1D). Both the average number of surface tumor nodules per liver and histological liver tumor incidence were negatively associated with T_3 status in mice, further supporting the HCC tumor suppressor activity of the thyroid hormone.

Development of HCC is considered as a process of chronic hepatic damage and inflammation. Therefore, we examined whether T_3 affects DEN-induced hepatotoxicity, DNA damage and inflammation during HCC development. The serum level of GPT (glutamic pyruvic transaminase, soluble), a classical marker of liver injury, was decreased in DEN-treated hyperthyroid mice for 17 wk (Fig. 1E). In addition, phospho-H2AFX/γ-H2AFX (phospho-H2A histone family, member X), a marker of the DNA damage response, revealed a significant decrease in the number of DNA-damaged hepatocytes in hyperthyroid mice (Fig. 1F, G). Expression of phospho-STAT3 (phospho-signal transducer and activator of transcription 3) and phospho-JUN/c-Jun (phospho-jun proto-oncogene), crucial inflammatory mediators promoting HCC, was increased in hypothyroid mice but decreased in hyperthyroid mice, compared with the euthyroid group (Fig. 1F). Clearly, T_3 protects liver cells against DEN-induced hepatotoxicity, DNA damage and inflammation, consequently suppressing tumor development.

T_3 triggers autophagy to attenuate DEN-induced HCC progression

Autophagy is hypothesized to suppress genomic instability and inhibit tumorigenesis through elimination of SQSTM1-associated protein aggregates and damaged organelles.[15] We further explored the role of T_3-triggered autophagy in tumor suppression using a mouse model of DEN-induced HCC. Following T_3 stimulation, expression of cleaved and lipidated microtubule-associated protein 1 light chain 3 (LC3-II) in THRA-overexpressing HepG2 and CL-48 hepatocyte cell lines was enhanced (Fig. 2A). Furthermore, increased LC3-II levels, in conjunction with SQSTM1 downregulation, were observed in livers of T_3-treated mice (Fig. 2B). Importantly, the higher molecular weights of SQSTM1 were detected in the liver extracts of hyperthyroid mice (Fig. 2B), an effect that was abolished after calf intestinal alkaline phosphatase (CIP) treatment (Fig. 2C). Thus, we hypothesize that T_3 promotes SQSTM1 phosphorylation and activates autophagy to stimulate the degradation pathway. Subsequently, chloroquine was utilized to clarify the role of T_3-triggered autophagy and lysosomal activity in tumor prevention. At 26 wk after initial DEN administration, liver tumor multiplicity and HCC incidence were increased in CQ-treated mice, compared with the control group. In contrast, almost no tumor nodules were detected in the hyperthyroid group. Notably, the tumor preventive effect of T_3 was blocked upon CQ administration (Fig. 2D, E). Histological staining of liver sections from these groups of mice confirmed the morphological features of HCC induced by DEN (Fig. 2F). Our results conclusively demonstrate that T_3 suppresses DEN-induced hepatocarcinogenesis through autophagy and lysosome-mediated degradation.

T_3 suppresses DEN-induced liver injury and DNA damage through autophagy

The carcinogenic capacity of DEN is attributed to its oxygen species (ROS) induction capability, which causes hepatic DNA damage and cytotoxicity.[16] As autophagy is regarded as an intracellular self-protection mechanism, we attempted to determine whether the hepatoprotective function of T_3 against DEN-induced toxicity is mediated through this process. After treatment with phosphate-buffered saline (PBS; euthyroid), T_3

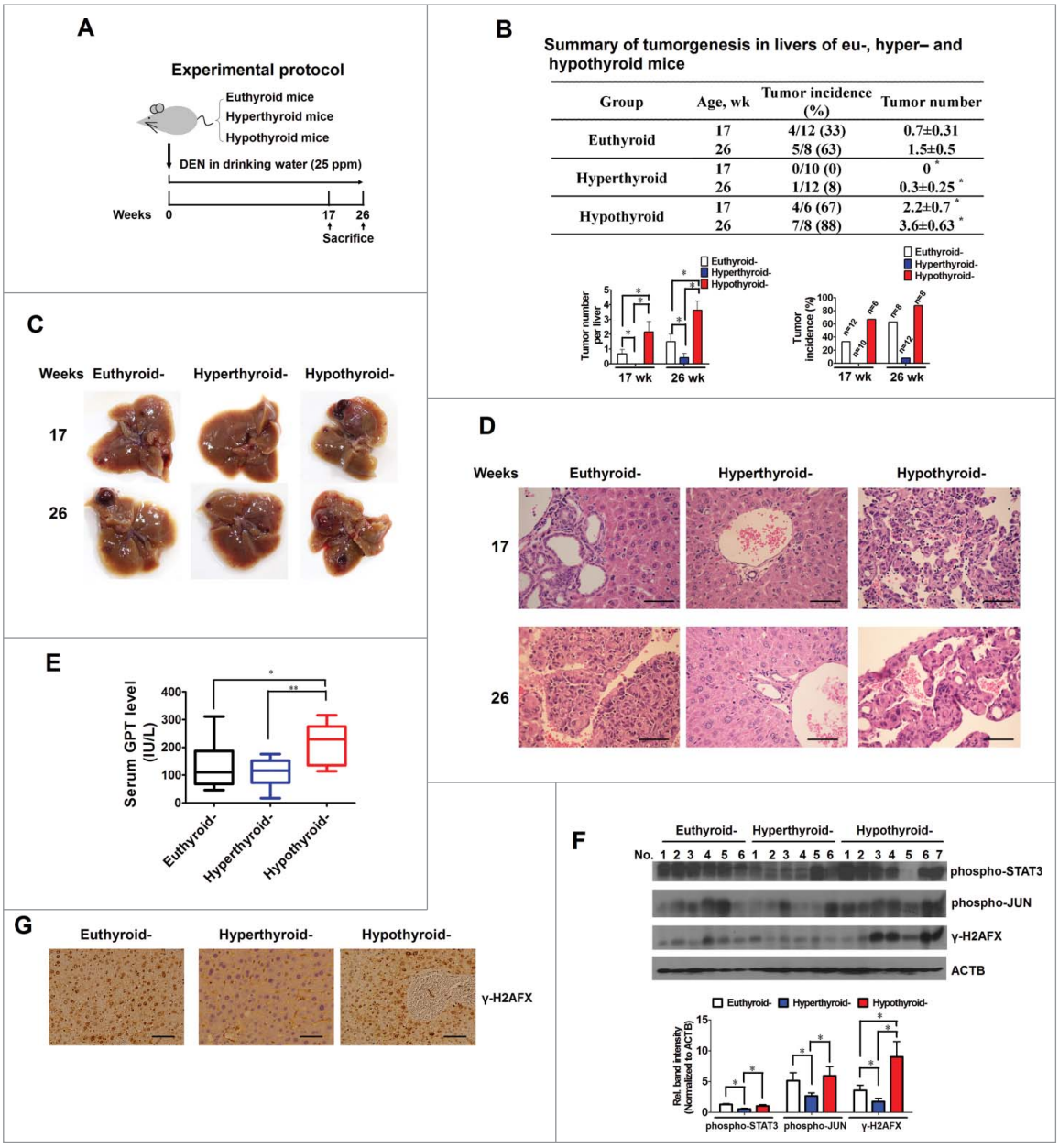

Figure 1. Thyroid hormone suppresses DEN-induced hepatocarcinogenesis in mice. (A) Diagram of the experimental protocol. (B) Hepatocellular carcinogenesis in the indicated groups of DEN-treated mice. Tumor number per liver and tumor incidence of these groups of mice are shown as bar graphs in the lower panels. Data are presented as means ± SD of each group, and differences statistically determined with the Student *t* test. *, $P > 0.05$ vs. euthyroid group. (C, D) Morphology of livers and representative images of H&E-stained liver sections from mice treated with DEN for 17 and 26 wk. Scale bar: 50 μm. (E) Serum GPT in the mice receiving DEN treatment for 17 wk. * and **, $P > 0.05$ and $P < 0.01$, respectively. (F) Immunoblot and densitometric analysis (lower panel) of hepatic levels of phospho-STAT3, phospho-JUN, and γ-H2AFX in the numbers of mice receiving DEN treatment for 17 wk. *, $P > 0.05$ (G) Representative IHC staining images of γ-H2AFX in liver sections from the indicated mouse groups after 17 wk of DEN treatment.

(hyperthyroid), CQ or CQ plus T_3 for 14 d, mice were subjected to DEN to induce hepatic damage. In the euthyroid group, serum GPT levels were significantly increased upon DEN treatment, but reduced after 2 d of exposure. In contrast, DEN had a minor effect on serum GPT levels in hyperthyroid mice. However, both groups receiving CQ exhibited higher serum GPT (Fig. 3A). T_3 treatment in mice repressed the expression of hepatic γ-H2AFX after exposure to DEN. CQ treatment not only promoted γ-H2AFX expression but also abolished the γ-H2AFX-suppressing effect of T_3 (Fig. 3B and Fig. S1). Additionally, histological analysis of liver sections from these groups of mice (2 d after DEN injection) revealed that compared to the control group, mice subjected to CQ treatment displayed features of severe liver injury, with necrosis and ballooning degeneration in increased numbers of hepatocytes. T_3 treatment effectively prevented the development of hepatic damage (Fig. 3C), whereas CQ antagonized this protective effect.

Adeno-associated virus (AAV) vectors are an efficient platform for delivery of RNA interference into liver.[17,18] To further determine whether the protective effect of T_3 is through autophagy, genetic inhibition of hepatic *Atg7* via adeno-associated virus serotype 8 (AAV8) vector-delivered shRNA in livers of eu- and hyper-thyroid mice was performed. As expected, knockdown of ATG7 promoted accumulation of SQSTM1 along with suppressed LC3-II production, indicating the inhibition of autophagy in mouse livers (Fig. 3D). Notably, higher

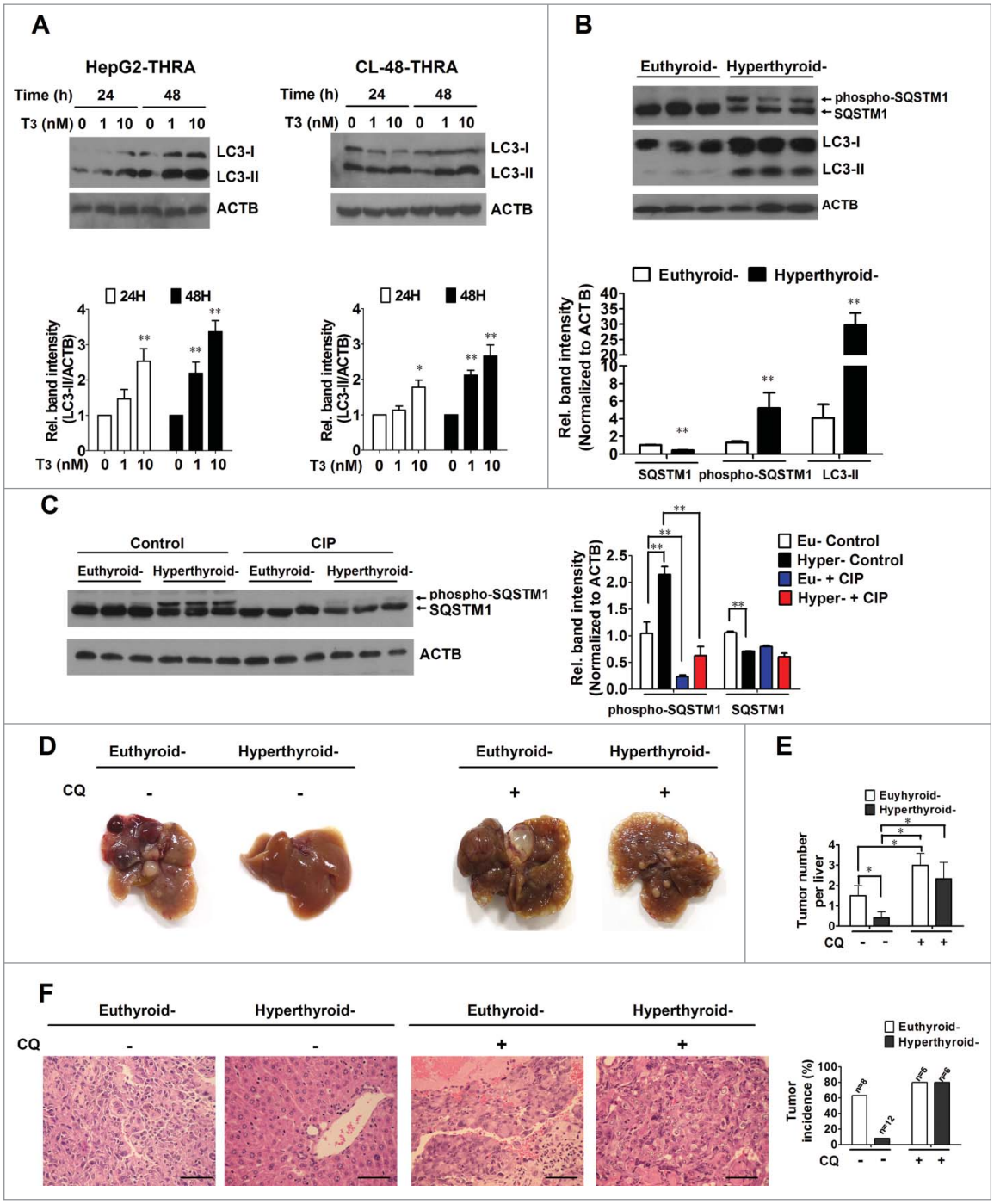

Figure 2. T_3-THRs induces autophagy to inhibit DEN-triggered hepatocarcinogenesis. (A) Immunoblot and densitometric analysis analysis (lower panel) of LC3-II levels in HepG2-THRA and CL-48-THRA cells treated with or without T_3 for the indicated times. Values are presented as fold expression relative to 0 nM T_3 at the indicated time-points. (N = 3, **, P>0.01). (B) Following intraperitoneal injection of T_3 (10 μg /100 g body weight) or PBS for 14 d, hepatic LC3-II and SQSTM1 levels of mice were determined using immunoblot and densitometric analysis (lower panel). (N = 3, **, $P > 0.01$). (C) After CIP treatment for 2 h, hepatic SQSTM1 proteins of euthyroid and hyperthyroid mice were determined via immunoblot and densitometric analysis (right panel). **, P>0.01 (D) Representative liver morphology of CQ or vehicle-treated euthyroid and hyperthyroid mice receiving DEN for 26 wk. Tumor number per liver (top panel) and tumor incidence (bottom panel) are shown in (E), and H&E-stained liver sections are shown in (F). Scale bar: 50 μm.

hepatic γ-H2AFX levels and serum GPT as well as more severe hepatic injury were observed in AAV8/Sh*Atg7*-treated mice after DEN challenge, whereas, knockdown of hepatic ATG7 in mice diminished the protective effect of T_3 (Fig. 3D to F and Fig. S2). Taken together, our findings clearly suggest that the protective effects of T_3 against DEN-induced DNA damage and liver injury are mediated through induction of autophagy.

T_3 regulates DAPK2 expression at the transcriptional level

To determine the specific roles of T_3-THRs signaling in HCC progression, clinical databases (Oncomine cancer microarray databases),[19,20] were searched in combination with previous oligomicroarray results derived from THRs-overexpressing HepG2 cells, with the aim of identifying critical THRs target genes implicated in autophagy. Among the several hundred

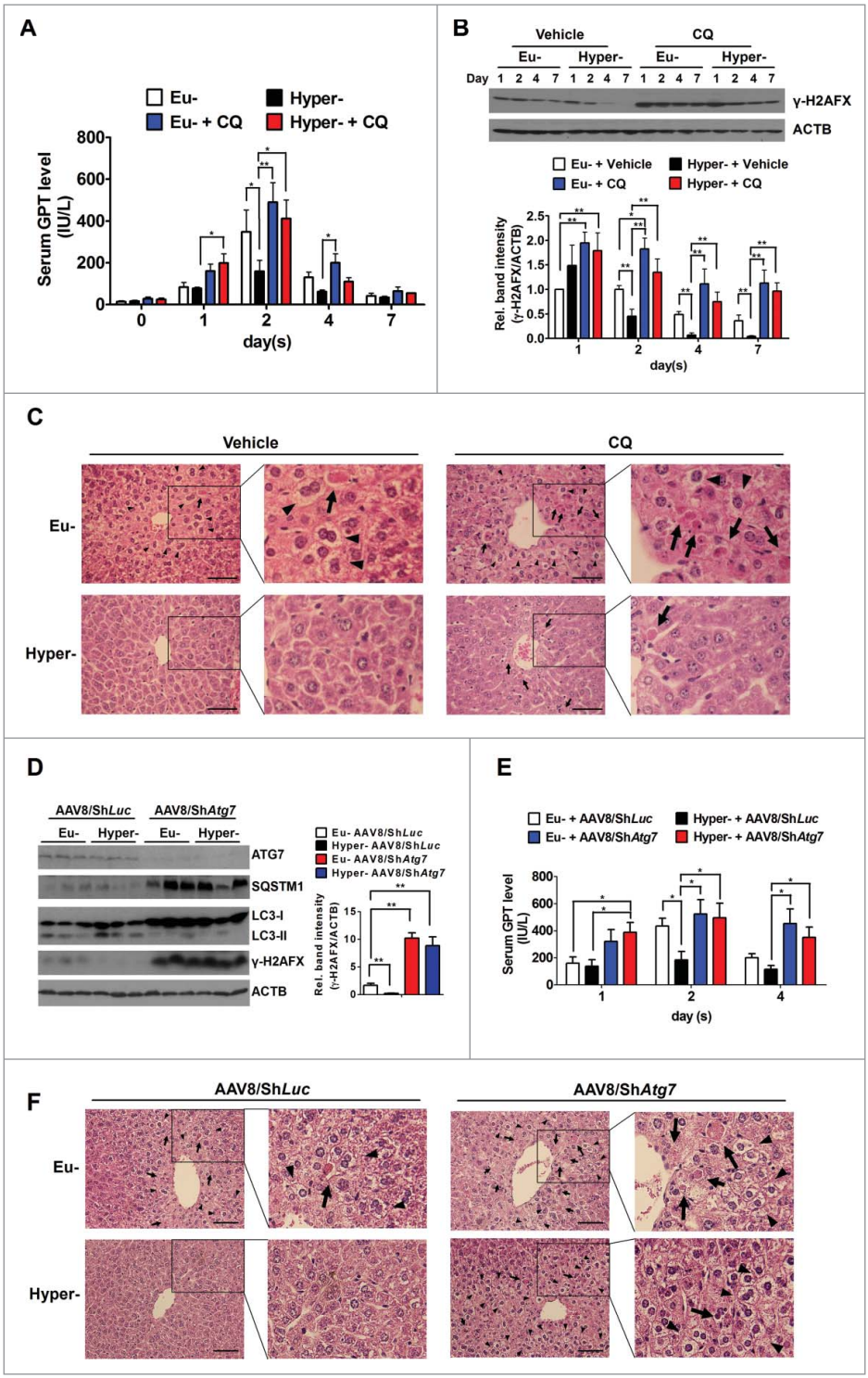

Figure 3. T_3-activated autophagy suppresses DEN-induced liver injury, DNA damage, and HCC progression. (A, E) Serum GPT levels of the indicated groups of mice were assessed on the indicated days after DEN injection (N $\geq$ 3 mice for each group). * and **: $P < 0.05$ and $P < 0.01$, respectively. (B) Liver γ-H2AFX expression levels of the indicated groups of mice were assessed 1, 2, 4 and 7 d after DEN injection. The relative folds of γ-H2AFX expression in these groups of mice are shown in the lower panel (N = 3, * and **, $P > 0.05$ and $P<0.01$, respectively). (C, F) Representative images of H&E-stained hepatic sections from the indicated mice 2 d after DEN injection. Arrows and arrowheads indicate hepatocytes with necrosis and ballooning degeneration, respectively. Scale bar: 50 μm. (D) Hepatic ATG7, SQSTM1, LC3-II and γ-H2AFX, expression levels of the indicated groups of mice were assessed 2 d after DEN injection (N = 3 for each group). The relative folds of γ-H2AFX expression in these groups of mice are shown in the right panel (N = 3, **, $P > 0.01$).

TR-targeted genes, *DAPK2* was selected owing to its clear involvement in autophagy. Within the datasets examined, *DAPK2* was highly stimulated by T_3-THRA signaling in HepG2 cells and positively correlated with *THRA* and *THRB* in clinical specimens (Fig. 4A). *DAPK2* mRNA and protein were induced by T_3 in a time-, dose- and THRs-dependent manner in various THR-overexpressing cell lines (Fig. 4B to D). Analogous effects of T_3 on DAPK2 were observed in CL-48, a normal hepatocyte cell line expressing exogenous THRA (Fig. 4D). To ascertain whether T_3 similarly induces *DAPK2* expression in

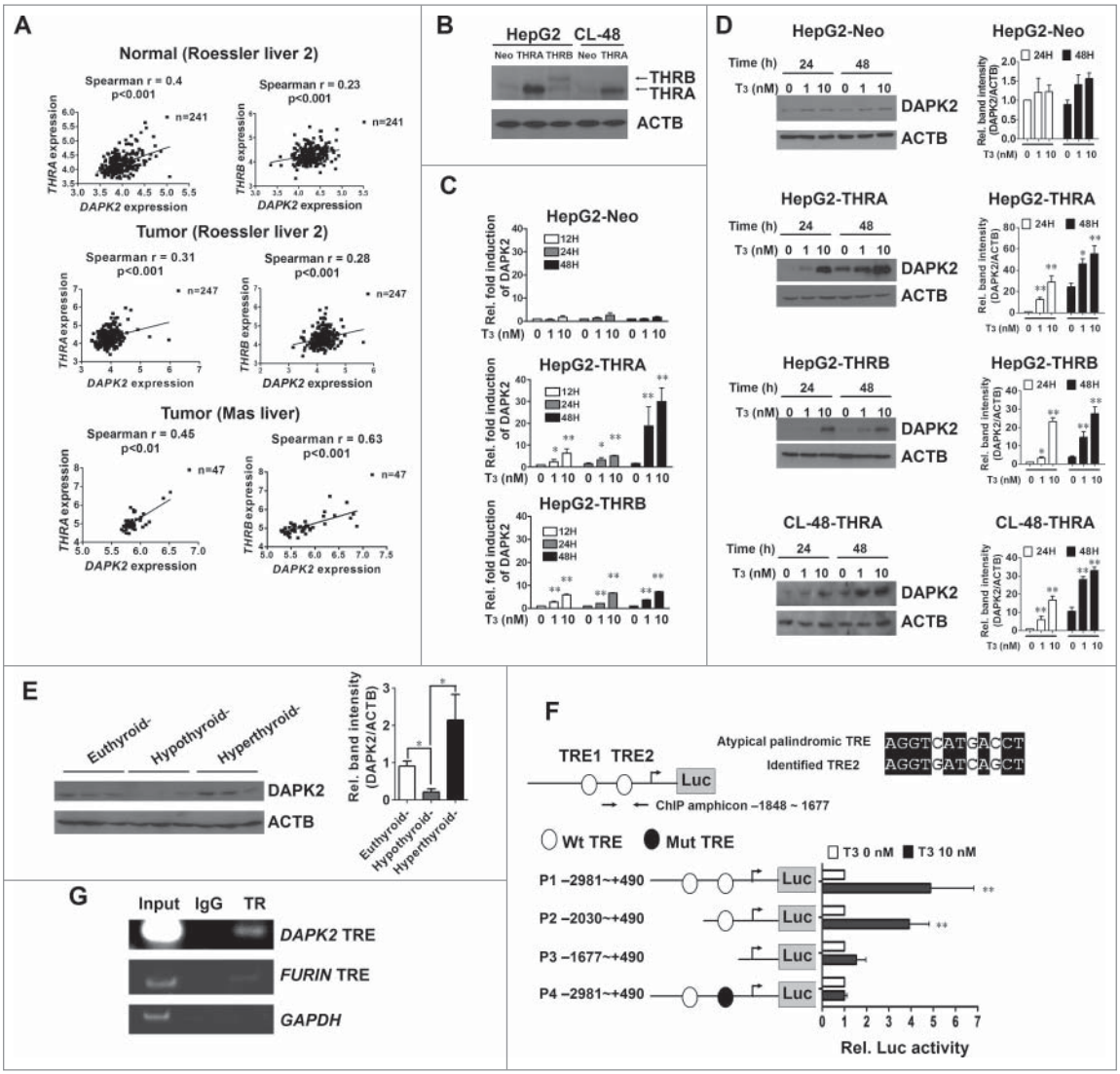

Figure 4. Effects of T_3 on *DAPK2* expression in hepatocytes. (A) Expression levels of *DAPK2, THRA* and *THRB* were retrieved from the published Oncomine data sets of Roessler liver 2 and Mas liver (GEO accession: GSE14520 and GSE14323 respectively). Spearman analysis of the plotted mRNA expression values revealed significant positive correlation of *DAPK2* expression with that of either THRA or THRB in normal and HCC specimens. (B) Western blot analysis of expression levels of THR proteins in several stably transfected cells carrying the indicated genes. (C) qRT-PCR analysis of the expression levels of *DAPK2* in HepG2 stably transfected cells treated with or without T_3 (1 or 10 nM) for 24 and 48 h. Values are presented as fold induction relative to 0 nM T_3 at the indicated time-points. * and **, $P > 0.05$ and $P > 0.01$, respectively. (D) Immunoblot and densitometric analysis (right panels) of the expression levels of DAPK2 in HepG2 or CL-48 stably transfected cells treated with or without T_3 (1 or 10 nM) for 24 and 48 h. Values are presented as fold expression relative to 0 nM T_3 at the indicated time-points. (N = 3, * and **, $P > 0.05$ and $P > 0.01$, respectively). (E) Immunoblot and densitometric analysis (right panel) of DAPK2 levels in euthyroid, hypothyroid and hyperthyroid mice (N = 3, *, $P > 0.05$). (F) Relative luciferase activity of various deletions or mutations of the *DAPK2* 5′-flanking region were determined in the HepG2-THRA cells after T_3 (0 or 10 nM) treatment for 24 h. The locations of putative TREs are presented as oval shapes in the 5′-flanking region. (G) ChIP assays showing that THRA is associated with TRE within the *DAPK2* promoter region. The location of the primer set for amplifying TRE within the DAPK2 promoter region is shown in the top diagram of (F). Promoters of *FURIN* and *GAPDH* served as positive and negative controls, respectively.

vivo, liver extracts of euthyroid, hyperthyroid and hypothyroid mice were analyzed. Consistent with the in vitro results, hepatic DAPK2 expression was upregulated in T_3-treated mice, compared to hypothyroid mice (Fig. 4E). Clearly, T_3 stimulates expression of *DAPK2* at both the mRNA and protein levels in vitro as well as in vivo.

To further determine whether T_3-THRs-mediated transcriptional activation is required for *DAPK2* induction, Serial 5′ deletion mutants of the *DAPK2* promoter were generated for identifying the bona fide TRE sequence interacting with T_3 (Fig. 4F, P1–P4). Sequence analysis revealed 2 putative thyroid response elements (TRE1 and 2). Interestingly, T_3 enhanced the transactivation activity of the fragments encompassing positions −2981 to +490 (P1) and −2030 to +490 (P2, TRE1-deleted mutant). However, the TRE2-deleted fragment (positions −1677 to +490, P3) lost T_3-induced promoter activity. Site-directed mutagenesis of TRE2 (P4) resulted in blockade of T_3-induced activity of the full-length promoter (Fig. 4E). The data collectively suggest that the transcriptional effect of T_3 on the *DAPK2* promoter is specifically mediated through interactions with TRE2 (positions −1771 to −1760). The sequence of TRE2, AGGTGATCAGCA, resembles an atypical palindromic TRE, and binding of THRA to this region was confirmed with the chromatin immunoprecipitation (ChIP) assay (Fig. 4G). These findings demonstrate that THRs bind physically to the *DAPK2* upstream element and promote its transcription upon T_3 stimulation.

T_3 promotes autophagy through DAPK2 induction

In view of the finding that T_3 simultaneously induces *DAPK2* expression and autophagy, we further investigated whether DAPK2 is responsible for T_3-triggered autophagy in liver cells. Ectopic expression of DAPK2 in HepG2 cells led to decreased SQSTM1 levels, and CQ treatment further promoted accumulation of LC3-II along with restored SQSTM1 expression in DAPK2-expressing cells (Fig. 5A). To further examine the effect of DAPK2 on autophagic flux, we analyzed the fluorescence signal in cells transfected with the tandem mRFP-GFP-*LC3B* reporter. In contrast to control HepG2 cells, ectopic expression of DAPK2 led to an increased proportion of vesicles displaying red fluorescence only, indicating induction of complete autophagy in liver cells (Fig. 5B).

The essential role of DAPK2 in T_3-induced autophagy was verified by shRNA- mediated *DAPK2* knockdown in HepG2-THRA cells (Fig. 5C). We found that although T_3 enhanced autophagic flux, as shown by the increased intensities of LC3-II in the presence of CQ, this effect on autophagy was blockaded in DAPK2-depleted cells (Fig. 5C). Furthermore, the T_3-stimulated number of RFP-LC3B-II punctate foci of the mRFP-GFP-*LC3B* tandem reporter was reduced after knockdown of DAPK2 (Fig. 5D). Based on these results, we propose that thyroid hormone-activated autophagy is predominantly mediated via *DAPK2* upregulation.

T_3 promotes autophagic clearance of ubiquitined proteins through DAPK2-mediated SQSTM1 phosphorylation

As SQSTM1 is a crucial mediator for clearance of aggregated proteins and damaged organelles in the autophagy system,[21] we thus asked whether T_3 and DAPK2 have any impact on the affinity of SQSTM1 for ubiquitinated proteins. To this end, in the presence of MG132 and CQ, HepG2-THRA cells were treated with T_3 and/or ectopically expressing DAPK2, and then SQSTM1 and associated proteins were collected by immunoprecipitation (IP). We found significantly higher levels of polyubiquitinated (poly-Ub) proteins associated with SQSTM1 in either T_3-THRA or DAPK2-treated cells (Fig. 6A, B). On the contrary, T_3-THRA induced SQSTM1 association with poly-Ub proteins and LC3-II proteins were diminished following knockdown of DAPK2 (Fig. 6C). These data were further corroborated by the immunofluorescence staining results, in which knockdown of DAPK2 blockaded T_3-stimulated colocalization of SQSTM1, poly-Ub aggregates, and EGFP-LC3B-II puncta in eGFP-*LC3B* transfected HepG2-THRA cells (Fig. 6D). Mounting evidence has suggested that phosphorylation of SQSTM1 regulates autophagic clearance of ubiquitinated proteins and protein aggregates.[22,23] As increased phosphorylation of SQSTM1 was observed in the livers of T_3-treated mice (Fig. 2B, C), it suggests that SQSTM1 might

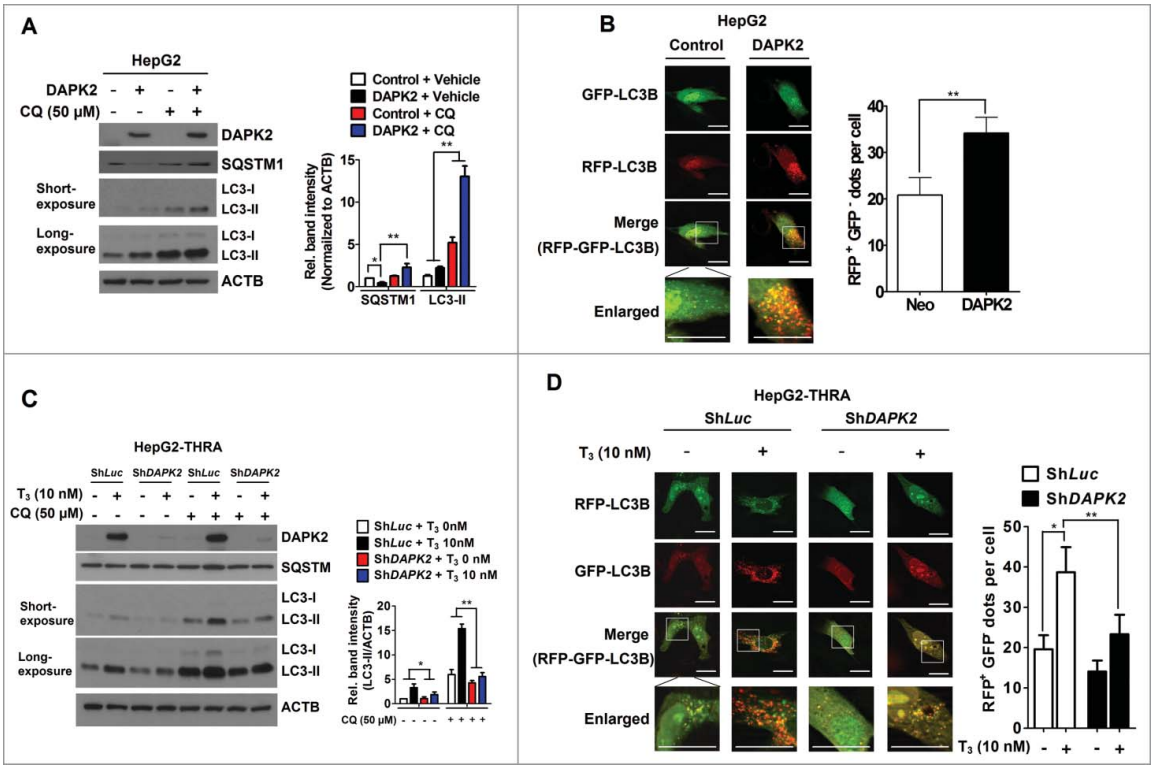

Figure 5. T_3 induces autophagy via DAPK2 in hepatic cells. (A) After stimulation with vehicle or CQ for 24 h, lysates of HepG2-DAPK2 or control cells were subjected to immunoblot for detection of DAPK2, SQSTM1 and LC3-II. The relative folds of SQSTM1 and LC3-II expression in these cells are shown in the right panel (N = 3, * and **, $P > 0.05$ and $P > 0.01$, respectively). (B) Visualization of autophagy flux in mRFP-GFP-*LC3B*-transfected HepG2-DAPK2 and control cells using fluorescence microscopy. (C) Immunoblot analysis of the expression patterns of DAPK2, SQSTM1 and LC3-II in T_3-stimulated HepG2-THRA cells with or without CQ treatment after infection with lentivirus expressing luciferase (Sh*Luc*) or *DAPK2*-targeting shRNA. The relative folds of LC3-II expression in these cells are shown in the right panel (N = 3, * and **, $P > 0.05$ and $P > 0.01$, respectively). (D) Autophagy flux in mRFP-GFP-*LC3B*-transfected HepG2-THRA-Sh*Luc* or HepG2-THRA-Sh*DAPK2* cells, in the presence or absence of T_3, was detected with fluorescence microscopy. Scale bar: 20 μm. The numbers of acidic vesicular LC3-II (RFP^+ GFP^- signal) per cell in (B) and (D) were calculated and shown in the right panels (* and **, $P > 0.05$ and $P > 0.01$, n = 10).

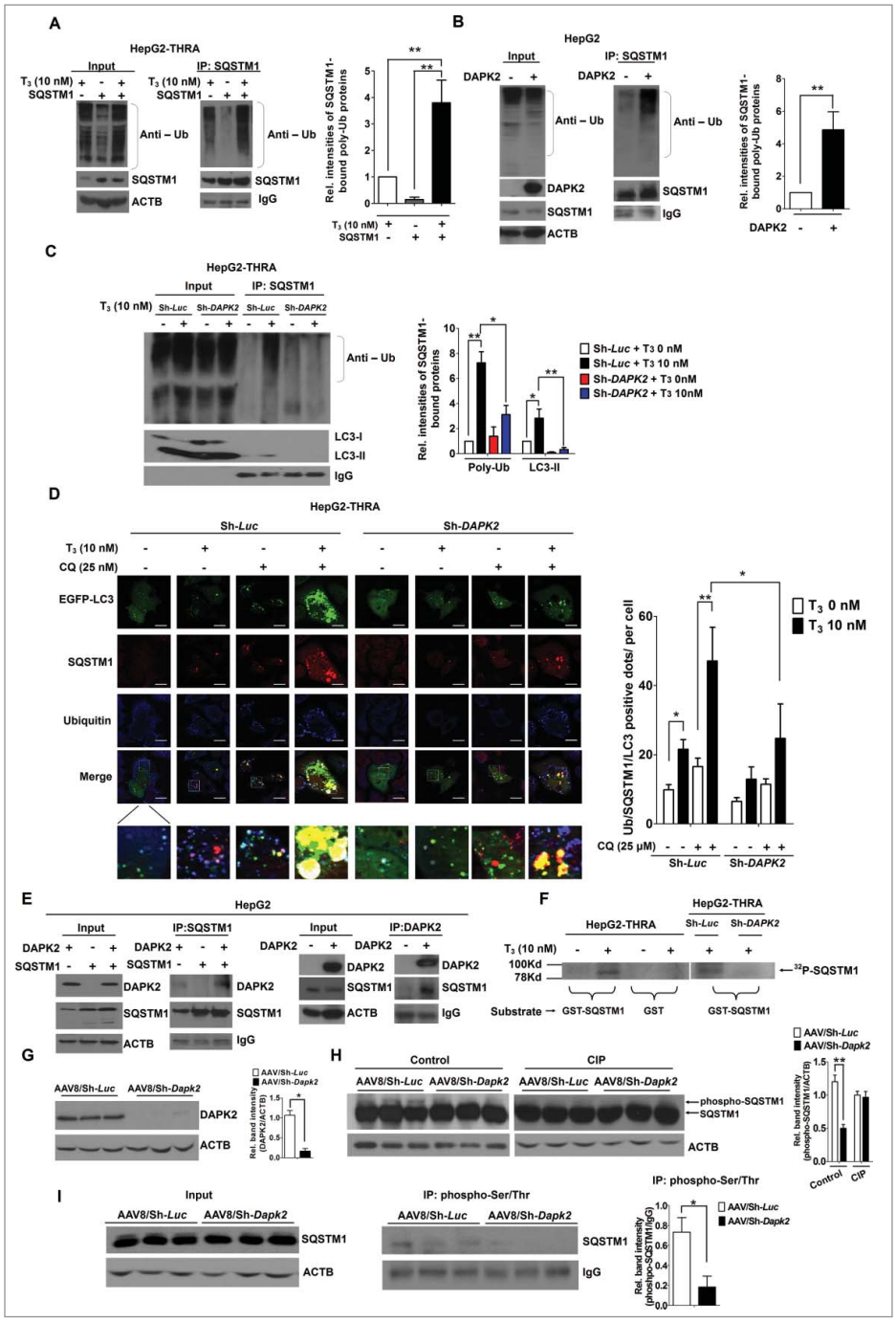

Figure 6. T3 promotes phosphorylation of SQSTM1 to regulate selective autophagy via DAPK2 in hepatic cells. ((A)to C) T_3 enhances binding between SQSTM1 and poly-Ub proteins through DAPK2. After stimulation of MG132 (5 μM) and CQ (25 μM) for 8 h, lysates of T_3-THRA- or DAPK2-treated cells, or T_3-stimulated HepG2-THRA-sh*Luc* and HepG2-THRA-sh*DAPK2* cells were extracted to measure the expression (input) of the indicated proteins, or subsequently subjected to IP using an anti-SQSTM1 antibody. Immunoblot analysis with the indicated antibodies was performed. The relative folds of SQSTM1-bound poly-Ub proteins or LC3-II normalized to IgG in these cells are shown in the right panels (N = 3, * and **, $P > 0.05$ and $P > 0.01$, respectively). (D) eGFP-*LC3B*-transfected DAPK2 knocked- down HepG2-THRA cells were cultured in the absence or presence of 10 nM T_3 for 24 h. CQ was added for a further 8 h, as indicated. Subsequently, IF staining of SQSTM1, poly-Ub proteins and EGFP-LC3 was performed. Right, the number of SQSTM1, poly-Ub, and EGFP-LC3-positive dots per cell was calculated (*, $P < 0.05$; **, $P < 0.01$, n = 3). Scale bar: 20 μm. (E) CoIP of DAPK2 and SQSTMQ from HepG2 cells. Protein lysates of DAPK2-treated or SQSTM1-treated HepG2 cells were extracted to measure the expression (input) of the indicated proteins or subsequently subjected to IP using the anti-SQSTM1 or anti-DAPK2 antibodies. Immunoprecipitated SQSTM1 and DAPK2 were visualized by immunoblotting. (F) GST-SQSTM1 and GST proteins were incubated with immunopurified DAPK2 from control or DAPK2 depleted HepG2-THRA cells treated with or without T_3 in a kinase reaction mixture containing γ-^{32}P-ATP. The phospho-SQSTM1 (^{32}P-SQSTM1) fractions are indicated. (G) Immunoblot and densitometric analysis of DAPK2 in the livers of AAV8-infected mice (N = 3, **, $P > 0.01$). (H) After CIP treatment for 2 h, hepatic SQSTM1 proteins of AAV8/Sh*Luc* and AAV8/Sh*Dapk2*-infected mice were determined using immunoblot analysis. The relative folds of phospho-SQSTM1 in control or CIP treated hepatic extracts are shown in the right panel (N = 3, **, $P > 0.01$). (I) Hepatic lysates of AAV8/Sh*Luc* and AAV8/Sh*Dapk2*-infused mice were extracted to measure the expression (input) of the indicated proteins, or subjected to immunoprecipitation using a phospho-Ser/Thr antibody and subsequently analyzed with immunoblot using an anti-SQSTM1 antibody. The relative folds of immunoprecipitated-SQSTM1 normalized to IgG in these hepatic extracts are shown in the right panel (N = 3, **, $P > 0.01$).

be a novel target of DAPK2. Accordingly, we examined whether DAPK2 could interact and subsequently phosphorylate SQSTM1 to regulate its activity. Using co-immunoprecipitation assays (CoIP), we found that DAPK2 interacted with SQSTM1 in HepG2 cells in a by T_3-THRA dependent manner (Fig. 6E and Fig. S3). The

phosphorylation of SQSTM1 by DAPK2 was further demonstrated by an in vitro kinase assay with purified GST (glutathione S-transferase)-tagged SQSTM1 proteins and immunoprecipitated DAPK2 (Fig. 6F).

To determine the effect of DAPK2 on SQSTM1 phosphorylation in vivo, the AAV8-mediated knockdown of DAPK2 in liver was performed (Fig. 6G). Our results indicate that the levels of phospho-SQSTM1 were repressed in the livers of AAV8/Sh*Dapk2*-transduced mice (Fig. 6H). Notably, the level of the Ser/Thr phosphorylation of SQSTM1 was also reduced in livers of the AAV8/Sh*Dapk2*-transduced mice, which was consistent with the Ser/Thr kinase function of DAPK2 (Fig. 6I). Collectively, these findings suggest that T_3 induces SQSTM1 phosphorylation through activating DAPK2, leading to enhanced autophagic clearance of ubiquitinated proteins.

DAPK2 attenuates DEN-induced liver injury and DNA damage though induction of autophagy

In view of the above results demonstrating an autophagy-mediated protective effect of T_3 on DEN-induced hepatic DNA damage, inflammation, and liver injury, it was of interest to determine whether T_3-induced DAPK2 also participates in the protection of DEN-challenged liver.

Liver is a major target organ for gene delivery due to its high biosynthetic capacity and access to the bloodstream.[24] The adenoviral vector-mediated system is highly efficient for in vivo gene transfer to the liver.[25] In our experiments, mice were infused with GFP-expressing-adenoviruses carrying the *DAPK2* gene (Ad-*DAPK2*) or control (Ad-Control) via their tail veins, and subsequently subjected to DEN treatment. The adenovirus-infected livers exhibited GFP-positive hepatocytes (Fig. 7A). Higher DAPK2 and LC3-II levels were evident in livers of mice infused with Ad-*DAPK2* (Fig. 7B). Consistently, overexpression in livers led to significant attenuation of DEN-induced hepatic injury, characterized by necrosis and ballooning degeneration of hepatocytes (Fig. 7C). To further clarify the protective effect of DAPK2-induced autophagy on DEN-induced cytotoxicity in liver cells ex vivo, primary hepatocytes were isolated. Following Ad-*DAPK2* infection, primary hepatocytes displayed higher DAPK2 expression (Fig. 7D). At 48 h after transient stimulation with DEN, γ-H2AFX accumulation was observed in hepatocytes (Fig. 7E, F).

Administration of CQ further enhanced γ-H2AFX expression. Notably, DEN-triggered γ-H2AFX induction was suppressed in Ad-*DAPK2*-transduced primary hepatocytes, whereas γ-H2AFX expression was retained upon inhibition of DAPK2-induced autophagy by CQ (Fig. 7E, F). Further analysis of DNA damage using the APODNA-2 antibody recognizing fragmented single-stranded DNA revealed that ectopic expression of DAPK2 suppresses DEN-induced cytotoxicity in hepatocytes while administration of CQ inhibits the protective effect of DAPK2 (Fig. 7F). Next, mice were infused with AAV8/Sh*Dapk2* to determine whether the protective effect of T_3 against DEN is through DAPK2. The results shown that knockdown of DAPK2 not only caused higher γ-H2AFX expression, serum GPT levels and more severe injury in livers, but also abolished the protective effect of T_3 after DEN challenge (Fig. 7G to I, and Fig. S4). Taken together, the data suggest that T_3-induced DAPK2 significantly suppresses DEN-induced DNA damage and liver injury through activation of autophagy, supporting its potential function as a tumor suppressor in HCC.

The THRs-DAPK2 axis is downregulated in HCC

To determine the clinical significance of the TR-DAPK2 axis in HCC patients, we performed immunohistochemistry (IHC) staining of THRs and DAPK2 in 86 and 81 pairs of HCC histological sections, respectively. Tumor cells exhibited lower expression of THRs and DAPK2 whereas relatively strong staining was observed in the adjacent noncancerous regions (Fig. 8A, B). The THRs and DAPK2 expression patterns in these tumor specimens were classified into groups ranging from weak to strongly positive (Fig. 8C). The correlation between THRs and DAPK2 expression levels in these specimens was examined with Spearman analysis performed on the plotted IHC scores. We observed significant moderate correlation in 66 pairs of consecutive clinical specimens (Fig. 8D).

The correlation between DAPK2 and the autophagy pathway in HCC was additionally analyzed. In total, 54 consecutive specimens from patients with HCC were submitted for immunoblot detection of DAPK2 and SQSTM1 expression. Similar to the IHC results, the DAPK2 protein was downregulated in 68.5% (37 of 54) HCC cancerous tissues, compared to matched adjacent noncancerous tissues. Furthermore, the decrease in DAPK2 expression was accompanied by a concomitant increase in SQSTM1 levels in matched cancerous tissues in 50% (27 of 54) samples, compared with the adjacent noncancerous regions. The correlation between DAPK2 and SQSTM1 expression was analyzed using the tumor parts/nontumor parts (T/N) ratio of DAPK2 as a dependent variable. Linear regression analysis showed a negative correlation with the SQSTM1 T/N ratio (regression coefficient = −0.47; 95% confidence interval [CI], 0.926-0.003; $P < 0.05$). The results from 12 representative paired HCC specimens are shown in Figure 8E. Spearman analysis performed on the T/N ratios of DAPK2 and SQSTM1 revealed a moderate, but significant negative correlation (Fig. 8F). These results conclusively suggest that the THRs-DAPK2-autophagy axis is downregulated in HCC tumors.

Discussion

Accumulating evidence over the past few decades has supported the theory that blockade of cellular TH-THRs signaling causes a spectrum of liver-associated diseases ranging from hepatic steatosis to HCC.[1] Moreover, several studies have identified a close association between human neoplasia and aberrant *THRs* mutation or expression.[26,27] However, the specific roles of TH-THRs in hepatocarcinogenesis remain debatable. For example, recent studies report that THRs act as potent suppressors of tumor metastasis in breast cancer cell lines.[28] Moreover, THRs exert diverse activities at different stages of tumorigenesis. The same group further shows that double-knockout *thra thrb* mice are vulnerable to epithelial tumors, and THR deficiency suppresses the number of benign tumors

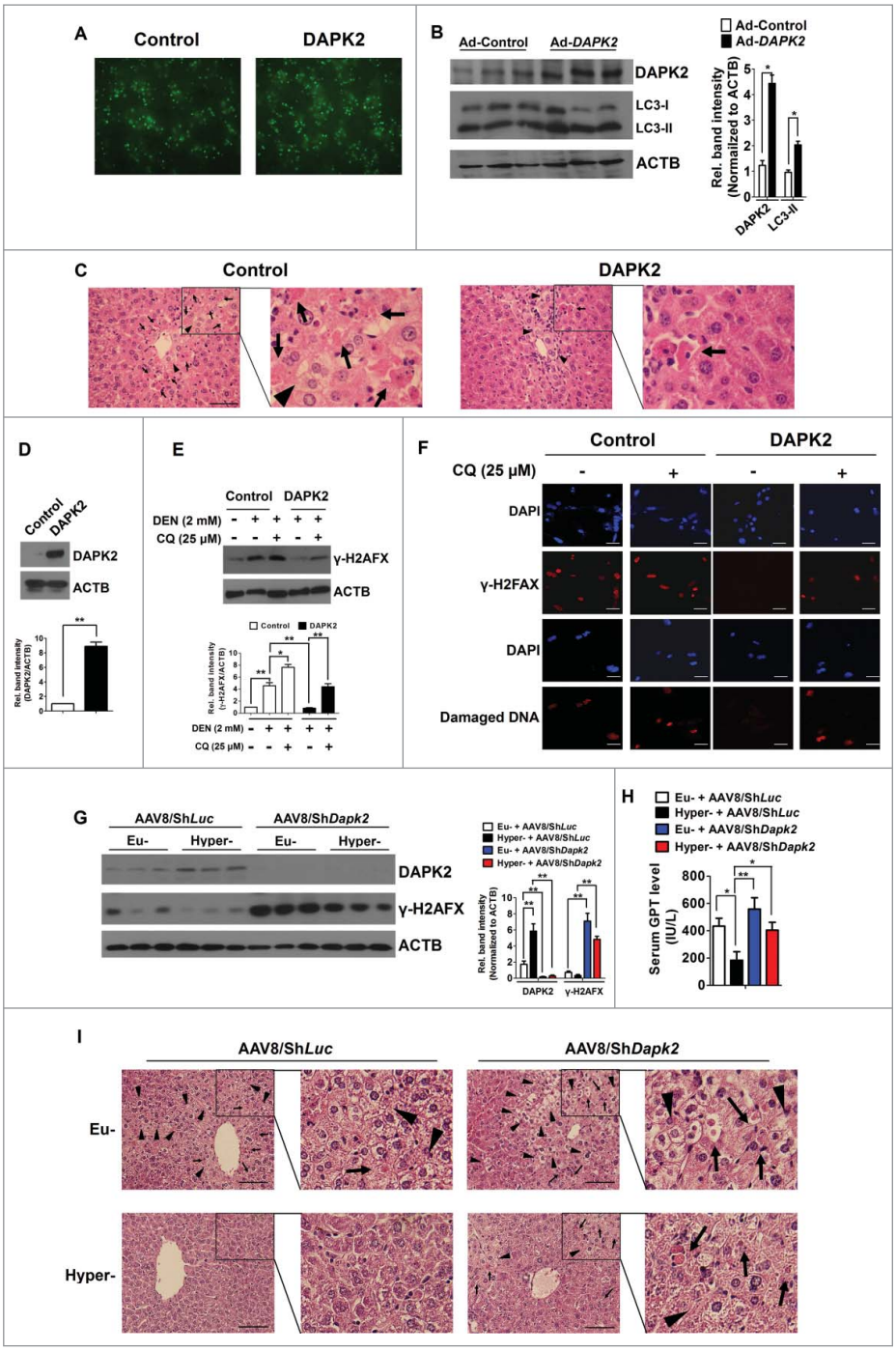

Figure 7. DAPK2-induced autophagy suppresses DEN-induced genomic damage and cell death in hepatic cells. After being infused with control (Ad-Control) or DAPK2-expressing (Ad-DAPK2) adenovirus (2×10^{11} viral particles/mouse) for 2 d, mice (N = 3) were treated with DEN (100 mg/kg) via peritoneal injection. Liver tissues were collected and subsequently subjected to immunoblot analysis and histological staining after 2 d. (A) Fluroescence image of livers of Ad-Control or Ad-*DAPK2*-treated mice. (B) Immunoblot and densitometric analysis (right panel) of DAPK2 and LC3-II expression patterns in livers of mice. (N = 3, *, $P > 0.05$) (C) H&E staining of liver sections from Ad-Control and Ad-DAPK2-infused mice after DEN exposure. Arrows and arrowheads indicate hepatocytes with necrosis and ballooning degeneration, respectively. Scale bar: 20 μm. (D) Primary hepatocyte cultures prepared from C57BL/6 mice were infected with Ad-control or Ad-DAPK2, and DAPK2 expression determined via immunoblot and densitometric analysis (lower panel). (N = 3, *, $P > 0.05$) (E, F) After DEN (2 mM) treatment for 24 h, Ad-Control or Ad-DAPK2-infected primary hepatocytes were cultured in hepatocyte maintenance medium with or without CQ (25 μM) for a further 24 h. Expression of γ-H2AFX was determined using immunoblotting and immunofluorescence. The relative folds of hepatic γ-H2AFX expression in these cells are shown in the lower panel of (E) (N = 3, **, $P > 0.01$). Damaged DNA in cells was detected with an antibody (APODNA-2) recognizing fragmented single-stranded DNA. Scale bar: 20 μm. (G) Hepatic DAPK2 and γ-H2AFX expression levels of the indicated groups of mice were assessed 2 d after DEN injection. The relative folds of hepatic DAPK2 and γ-H2AFX expression in these groups of mice are shown in the right panel (N = 3, **, $P > 0.01$). (H) Serum GPT levels of the indicated groups of mice assessed 2 d after DEN injection. (I) Representative images of H&E-stained hepatic sections from the indicated mice 2 d after DEN injection. Arrows and arrowheads indicate hepatocytes with necrosis and ballooning degeneration, respectively. Scale bar: 50 μm.

but enhances malignant tumor formation during carcinogenesis.

Intriguingly, the proposed tumor suppressor role of THRs remains a controversial issue. The divergent functions of T_3-THRs in tumor progression may be attributed to the differences in target organs and specific microenvironments of tumors at different stages. For instance, previous studies suggested that TH suppresses cellular growth of cancer cells via controlling

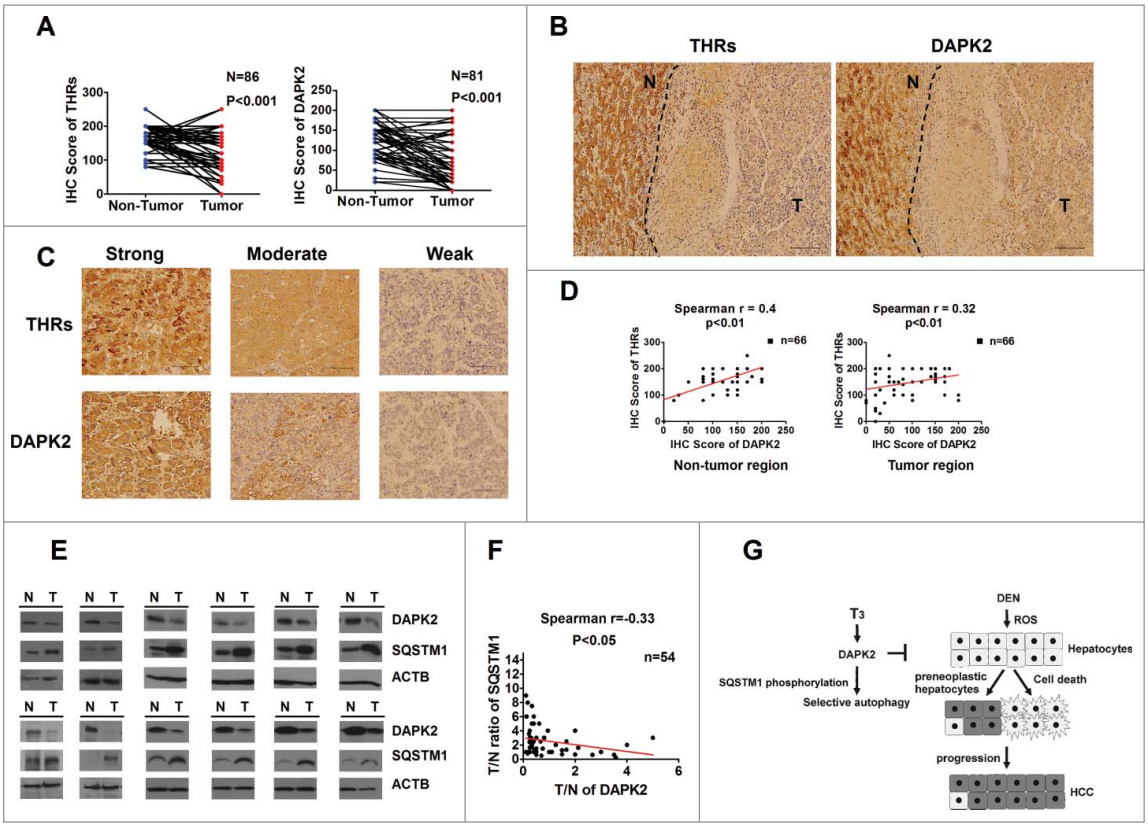

Figure 8. The THR-DAPK2 axis is downregulated in human malignant HCC. IHC staining of DAPK2 and THRs expression patterns in HCC specimens. (A) Paired scores of the intensities of DAPK2 and THRs expression in cancerous and adjacent noncancerous regions. Statistical significance was examined with the Student *t* test. (B) Representative IHC images of a HCC specimen containing tumor (T) and adjacent nontumor (N) regions stained with anti-THRs (left panel) or anti-DAPK2 antibody (right panel). Scale bar: 50 μm. (C) Representative IHC images showing strong, moderate and weak expression of DAPK2 and THRs expression in HCC tissues. (D) IHC scores of DAPK2 and THRs expression levels in tumor (right panel) and adjacent nontumor (left panel) regions are shown independently in scatter charts. Spearman rank correlation coefficients between IHC scores of DAPK2 and THRs in 66 pairs of consecutive clinical specimens among the HCC samples presented in (A) were analyzed. (E) Representative immunoblots of DAPK2 and SQSTM1 proteins in cancerous (T) and matched adjacent noncancerous tissues (N) from 12 patients. (F) The T/N ratios of DAPK2 and SQSTM1 proteins in each specimen were plotted in a scatter chart and their correlations examined using the Spearman coefficient. (G) A hypothetical model showing that DAPK2-mediated phosphorylation of SQSTM1 promotes selective autophagy and suppress hepatocarcinogenesis by thyroid hormone.

the expression of cell cycle regulators, such as phospho-RB1 (phospho-retinoblastoma 1), CCNE1 (cyclin E1) and CDK2 (cyclin-dependent kinase 2). However, in apoptosis-resistant hepatoma cells, T_3-THR signaling promotes tumor cell metastasis via upregulation of several extracellular matrix proteases.[29,30] Thus, further studies are warranted to clarify the specific functions of signaling through T_3-THRs in the processes of HCC development.

In the current study, an in vivo experimental system based on long-term administration of DEN in mice was developed. Using this system, we found that disruption of TH signals enhances HCC development to a significant extent. Conversely, T_3 exerted a suppressive effect on liver tumor development in mice. Accumulating evidence has suggested an inhibitory effect of autophagy on liver tumor initiation.[6] Our results collectively indicate that DAPK2-driven selective autophagy via SQSTM1 phosphorylation inhibits DEN-induced DNA damage and hepatic injury, which consequently prevents HCC development (Fig. 8G), and provide strong evidence linking the phenomena of decreased THRs and DAPK2 levels in hepatic tumor with HCC progression.

In liver, DEN is metabolized into an alkylating agent by several P450 isozymes, which induce DNA damage. Moreover, hepatic bioactivation of DEN generates a substantial amount of ROS potentially reacting with various biomolecules, such as nucleic acids, proteins, and lipids,[31,32] which are implicated in cellular organelle damage. In addition, ROS may activate inflammation-related signals, including MAPK8 (mitogen-activated protein kinase 8) and STAT3, which are frequently activated in human HCCs, especially aggressive tumors with poor prognosis.[33] Inhibition of autophagy in DEN-treated liver cells causes further ROS accumulation, accompanied by accelerated DNA damage and hepatic injury.[34] Increased oxidative stress is thought to occur due to the accumulation of SQSTM1-associated protein aggresomes and damaged organelles. Activation of autophagy leads to clearance of SQSTM1-associated aggresomes and reduction of ROS. We have shown that T_3 triggers SQSTM1 phosphorylation and promotes clearance of poly-Ub proteins and damaged organelles; consequently, attenuates DEN-induced DNA damage and hepatic injury in mice but also suppresses the STAT3 and MAPK8 pathway. DAPK2 was originally identified as an apoptotic trigger.[7] The majority of DAPK2-related research to date has focused on its cell-killing ability in cancer cells. However, the biological mechanism underlying its physiological significance has not been extensively investigated. Results from the current study suggest that rather than inducing cell death via apoptosis, DAPK2 triggers the autophagic process in hepatocytes. Upon efficient gene

delivery into liver of mice via intravenous infusion of adenoviruses, DAPK2-activated selective autophagy led to reduction of both genomic instability and liver injury immediately after DEN exposure.

Mice with hypothyroidism display lower hepatic DAPK2 expression and higher levels of genomic instability, and therefore have greater potential to generate tumor precursor cells that later develop into visible tumor foci in a few months. For tumor precursor cells to evolve into HCC, multiple rounds of mitosis are required, which cause genomic instability and generate greater oxidative stress.[35] T_3 supplementation in mice induces higher DAPK2 expression. Consequently, DAPK2-driven selective autophagy eliminates the accumulation of damaged DNA or oxidative stress-caused hepatic injury through SQSTM1 phosphorylation. Accordingly, we conclude that signaling by T_3-THRs upregulates DAPK2 to suppress HCC development through selective autophagy.

In summary, our proof-of-concept experiments suggest that application of T_3 constitutes an effective novel therapeutic option for chronic liver diseases, such as HCC.

Patients, materials and methods

Animal model of hepatocarcinogenesis

To induce hypothyroidism in 4-wk-old C57BL/6 male mice, 0.02% methimazole plus 0.1% sodium perchlorate was added to drinking water. Hyperthyroidism was induced in mice by treatment of drinking water with T_3 (2.5 mg/L every 2 wk).

For autophagy inhibition, mice from different thyroid groups received 50 mg/kg of CQ (Santa Cruz Biotechnology, sc-205629) via intraperitoneal injection once every 3 d. Two wk after thyroid manipulation and CQ injection, DEN (25 ppm, Sigma-Aldrich, N0258) was added to drinking water of the indicated groups of mice to induce HCC. Control mice were treated with PBS (137 mM NaCl [Sigma-Aldrich, S5150], 8 mM Na_2HPO_4 [Sigma-Aldrich, S5136], 2.7 mM KCl [Sigma-Aldrich, P5405], 1.5 mM KH_2PO_4 [Sigma-Aldrich, P5655], pH 7.4) Mice were sacrificed at 17 or 26 wk after initiation of DEN treatment.

To examine whether T_3-activated autophagy could suppresses DEN-induced liver injury and DNA damage. Mice were treated with T_3 (10 μg/100 g body weight), CQ (50 mg/kg) or T_3 plus CQ for 14 d before intraperitoneal injection of DEN (100 mg/kg). All groups of mice also received continued T_3 or CQ treatment after DEN injection. To further determine whether the protective effect of T_3 is through the DAPK2-autophagy axis, the mice received a single intravenous injection of 10^{12} vector genomes of AAV8/Sh-*Luciferase* (Sh*Luc*), AAV8/Sh*Atg7* or AAV8/Sh*Dapk2* and were subjected to T_3 treatment for 14 d. After DEN injection, liver tissues and serum of these mice were collected on various days. The construction and production of these pseudotyped AAV8 vectors, which contain the H1 promoter and the shRNA coding sequence, has been reported previously.[18] To determine the T_3 effect on DAPK2 expression in vivo, hyperthyroid mice were generated via intraperitoneal injection of T_3(10 μg/100 g body weight) for 14 d. To induce hypothyroidism in mice, 0.02% methimazole plus 0.1% sodium perchlorate was added to drinking water for 14 d. After sacrifice, total serum and livers were collected. Grossly visible liver tumors were measured with calipers and counted. Tissues were either fixed in 10% neutral-buffered formalin or stored at −80°C following standard protocols. Serum GPT levels were examined using a Fuji DRICHEM 55500 V analyzer (Fuji Medical System, Tokyo, Japan) following the manufacturer's instructions. All procedures were performed in accordance with the Guide for Care and Use of Laboratory Animals issued by the Institutional Animal Care and Use Committee of Chang Gung University and the National Institutes of Health of United States.

Cell cultures

All cells were maintained at 37°C in a humidified atmosphere of 5% CO_2 and 95% air. Human hepatocyte cell lines, including HepG2 and CL-48, were routinely cultured in Dulbecco's modified Eagle's medium (Invitrogen, 12800082) supplemented with 10% fetal bovine serum. Primary hepatocytes were isolated from 8-wk-old C57BL/6 male mice using the collagenase perfusion method. Cells were maintained in 10% fetal bovine serum-supplemented hepatocyte maintenance medium (Corning, 40-550-CV). For analysis of the gene function in human or mouse hepatocytes, adenovirus was added to the medium at a multiplicity of infection of 20 and cells infected for 6 h. T_3-depleted serum (T_3 0 nM) was prepared by treatment with AG 1-X8 resin (Bio-Rad, 40-1451). T_3 was purchased from Sigma-Aldrich (T2752).

Reverse transcription and quantitative PCR (qRT-PCR)

Total RNA was extracted with TRIzol reagent (Invitrogen, 10296-028) and reverse-transcribed into cDNA with the Superscript II kit (Invitrogen, 18064-014), according to manufacturers' protocols. qRT-PCR was conducted in a total reaction volume of 15 μl containing 50 ng forward and reverse primers, cDNA template and 1× SYBR Green reaction mix (Applied Biosystems, 4309155). The qPCR reaction was performed on the ABI PRISM 7500 sequence detection system (Applied Biosystems, Foster City, CA, USA).

Immunoblot analysis

Total cell lysates were isolated and fractionated via SDS-PAGE on a 12.5% gel, and separated proteins transferred to PVDF membranes. Following blocking in 5% (w/v) nonfat dried milk, membranes were incubated with the appropriate primary and HRP-conjugated secondary antibodies. Immune complexes were detected via chemiluminescence using an ECL detection kit (Amersham, RPN2232) and visualized with X-ray film. The densitometric analysis was performed with Image Gauge software (Fuji Film) and the relative band intensity normalized to ACTB (actin β) and quantified with respect to the first band set to 1. The following antibodies were used: DAPK2 (Abcam, ab51601), LC3B (Cell Signaling Technology, 2775), SQSTM1 (Santa Cruz Biotechnology, sc-28359), ubiquitin (Santa Cruz Biotechnology, sc-8017), ATG7 (GeneTex, GTX113613), phospho-Ser/Thr (Abcam, ab17464,), ACTB (Chemicon, MAB1501R), phospho-STAT3 (Abcam, ab76315), phospho-

JUN (Abcam, ab79756), THRs (C4 clone from Dr. Sheue-yann Cheng at the National Cancer Institute). For detecting ubiquitinated proteins in T_3-treated and DAPK2-treated cells, protein lysates followed by immunoblotting with anti-ubiquitin and anti-SQSTM1 antibody, membranes were stripped and reprobed with anti-ACTB antibody to check for equal protein loading.

Reporter assay and chip analysis

HepG2-THRs cells were transfected with pGL3-basic reporters (0.2 μg; Promega, E1751) containing various fragments of *DAPK2* 5′ flanking sequences and SVβ plasmid (0.05 μg) and the LacZ/β-galactosidase (β galactosidase) expression vector to normalize transfection efficiency. Treated cells were lysed 48 h after transfection to measure luciferase and GLB1 activities.

The ChIP assay was performed as described previously.[29] Briefly, THRA-binding DNA fragments were immunoprecipitated with mouse anti-THRs monoclonal antibody. Immunoprecipitated DNA fragments were amplified using specific primer sets targeting the region (positions −1848 to −1677) flanking *DAPK2* TRE2 (positions −1771 to −1760). The TRE region of the *FURIN* (furin, paired basic amino acid cleaving enzyme) promoter was used as a positive control and *GAPDH* (glyceraldehyde-3-phosphate dehydrogenase) as a negative control.

Human HCC specimens

Hepatic sections and protein extracts of HCC patients were obtained from the Chang Gung Memorial Hospital medical research center for hematoxylin and eosin (H&E) and IHC stain and immunoblot analysis. HCC and adjacent noncancerous liver tissue samples were confirmed using H&E staining. The study protocol was approved by the Medical Ethics and Human Clinical Trial Committee at Chang-Gung Memorial Hospital (NO:99-3588B).

Immunofluorescence and immunohistochemical staining

For immunofluorescence analysis, cells were fixed with 4% paraformaldehyde, and subsequently incubated with the appropriate primary and secondary antibodies.

To examine the effects of T_3-THRs and DAPK2 on the autophagic process, we analyzed the fluorescence signal in cells transfected with the tandem RFP-GFP-*LC3B* reporter.

Both GFP and RFP proteins were stable in newly formed autophagosomes, and therefore, respective green and red fluorescence were observed. Upon acidification of autophagosomes via fusion with lysosomes (acidic autolysosome formation), GFP fluorescence was attenuated and only red fluorescence remained.[36] Images were acquired using a Zeiss Apotome fluorescence microscope and Axio vision Rel 4.8 software (Carl Zeiss, Gottingen, Germany).

Resected liver tissue was processed as paraffin sections and subjected to H&E staining or immunohistochemical analysis with the Bond-max Automated Immunostainer (Leica Microsystems, Wetzlar, Germany). THRs and DAPK2-positive tumor cells in the representative microscopic fields were scored independently by 2 experienced pathologists. The following antibodies were used: DAPK2 (Abcam, ab51601), THRs (C4 clone from Dr. Sheue-yann Cheng at the National Cancer Institute), and mouse anti-single stranded DNA antibody (Cell Technology, APODNA-2). eGFP-*LC3B* and mRFP-GFP-*LC3B* plasmid were kind gifts from Dr. Po-Yuan Ke at Chang-Gung University.

Statistical methodology

One-way analysis of variance was used to compare the results obtained for more than one treatment. The data were analyzed using means, standard deviations, one-way analysis of variance (ANOVA), and Tukey's post hoc test. The differences in data between the 2 groups were assessed with the Student *t* test. The correlation between the results obtained with the 2 different measurements analyzed with Spearman's test.

Abbreviations

AAV	adeno-associated virus
AAV8	adeno-associated virus serotype 8
ACTB	actin β
Ad	adenoviruses
Atg5	autophagy-related 5
Atg7	autophagy-related 7
ATRA	All-trans retinoic acid
CALM1	calmodulin 1
CCNE1	cyclin E1
CDK2	cyclin dependent kinase 2
ChIP	chromatin immunoprecipitation
CIP	calf intestinal alkaline phosphatase
CoIP	co-immunoprecipitation
CQ	chloroquine
DAPK2	death-associated protein kinase 2
DEN	diethylnitrosamine
FURIN	furin, paired basic amino acid cleaving enzyme
GAPDH	glyceraldehyde-3-phosphate dehydrogenase
GPT/ALT1	glutamic pyruvic transaminase, soluble
GST	glutathione S-transferase
HCC	hepatocellular carcinoma
H2AFX	H2A histone family, member X
H&E	hematoxylin and eosin
IFNG	interferon gamma
IHC	immunohistochemistry
IP	immunoprecipitation
LacZ/β-galactosidase	β galactosidase
JUN/c-Jun	Jun proto-oncogene
Luc	luciferase
MAPK8/JNK1	mitogen-activated protein kinase 8
MAP1LC3B/LC3B	microtubule-associated protein 1 light chain 3 β
MTORC1	mechanistic target of rapamycin (serine/threonine kinase) complex 1
PBS	phosphate-buffered saline
poly-Ub	polyubiquitinated
RB1	retinoblastoma 1

RPTOR	regulatory associated protein of MTOR, complex 1
qRT-PCR	reverse transcription and quantitative PCR
ROS	reactive oxygen species
SQSTM1	sequestosome 1
STAT3	signal transducer and activator of transcription 3
T_3	3, 3′5-triiodo-l-thyronine
TH	thyroid hormone
THR	thyroid hormone receptor
TNF	tumor necrosis factor
TRE	thyroid hormone response element
T/N	tumor parts/nontumor parts
Ub	ubiquitin

Disclosure of potential conflicts of interest

No potential conflicts of interest were disclosed.

Funding

This work was supported by grants from Chang Gung Memorial Hospital, Taoyuan, Taiwan (CMRPD180011, CMRPD180012, CMRPD180013, CMRPD1A0331, CMRPD1A0332, CMRPD1A0333, CMRPD1C0271, CMRPD1C0272, CMRPD1C0273, CRRPD1F0011, NMRPD1A0921, NMRPD1A0922, NMRPD1A0923, NMRPD1A1231, NMRPD1A1232, NMRPD1A1233) and from the Ministry of Science and Technology of the Republic of China (MOST 100-2320-B-182-029-MY3; 100-2321-B-182-005; 101-2321-B-182-003; 102-2321-B-182-003; 105-2321-B-182-002-MY3). We thank Shih-Hsien Chen and Jyh-Ping Chen for helping to isolate mice hepatocytes, Mi-Hua Tao for AAV8 producing. The authors have no conflicting financial interests.

References

[1] Lin YH, Huang YH, Wu MH, Wu SM, Chi HC, Liao CJ, Chen CY, Tseng YH, Tsai CY, Tsai MM, et al. Thyroid hormone suppresses cell proliferation through endoglin-mediated promotion of p21 stability. Oncogene 2013; 32:3904-14; PMID:23376845; http://dx.doi.org/10.1038/onc.2013.5

[2] Barlow C, Meister B, Lardelli M, Lendahl U, Vennstrom B. Thyroid abnormalities and hepatocellular carcinoma in mice transgenic for v-erbA. EMBO J 1994; 13:4241-50; PMID:7925269

[3] Hassan MM, Kaseb A, Li D, Patt YZ, Vauthey JN, Thomas MB, Curley SA, Spitz MR, Sherman SI, Abdalla EK, et al. Association between hypothyroidism and hepatocellular carcinoma: a case-control study in the United States. Hepatology 2009; 49:1563-70; PMID:19399911; http://dx.doi.org/10.1002/hep.22793

[4] Kuma A, Hatano M, Matsui M, Yamamoto A, Nakaya H, Yoshimori T, Ohsumi Y, Tokuhisa T, Mizushima N. The role of autophagy during the early neonatal starvation period. Nature 2004; 432:1032-6; PMID:15525940; http://dx.doi.org/10.1038/nature03029

[5] Komatsu M. Liver autophagy: physiology and pathology. J Biochem 2012; 152:5-15; PMID:22661765; http://dx.doi.org/10.1093/jb/mvs059

[6] Takamura A, Komatsu M, Hara T, Sakamoto A, Kishi C, Waguri S, Eishi Y, Hino O, Tanaka K, Mizushima N. Autophagy-deficient mice develop multiple liver tumors. Genes Dev 2011; 25:795-800; PMID:21498569; http://dx.doi.org/10.1101/gad.2016211

[7] Inbal B, Shani G, Cohen O, Kissil JL, Kimchi A. Death-associated protein kinase-related protein 1, a novel serine/threonine kinase involved in apoptosis. Mol Cell Biol 2000; 20:1044-54; PMID:10629061; http://dx.doi.org/10.1128/MCB.20.3.1044-1054.2000

[8] Inbal B, Bialik S, Sabanay I, Shani G, Kimchi A. DAP kinase and DRP-1 mediate membrane blebbing and the formation of autophagic vesicles during programmed cell death. J Cell Biol 2002; 157:455-68; PMID:11980920; http://dx.doi.org/10.1083/jcb.200109094

[9] Ber Y, Shiloh R, Gilad Y, Degani N, Bialik S, Kimchi A. DAPK2 is a novel regulator of mTORC1 activity and autophagy. Cell Death Differentiation 2015; 22:465-75; PMID:25361081; http://dx.doi.org/10.1038/cdd.2014.177

[10] Rizzi M, Tschan MP, Britschgi C, Britschgi A, Hugli B, Grob TJ, Leupin N, Mueller BU, Simon HU, Ziemiecki A, et al. The death-associated protein kinase 2 is up-regulated during normal myeloid differentiation and enhances neutrophil maturation in myeloid leukemic cells. J Leukoc Biol 2007; 81:1599-608; PMID:17347302; http://dx.doi.org/10.1189/jlb.0606400

[11] Tseng YH, Ke PY, Liao CJ, Wu SM, Chi HC, Tsai CY, Lin YH, Lin KH. Chromosome 19 open reading frame 80 is upregulated by thyroid hormone and modulates autophagy and lipid metabolism. Autophagy 2014; 10:20-31; PMID:24262987; http://dx.doi.org/10.4161/auto.26126

[12] Sinha RA, You SH, Zhou J, Siddique MM, Bay BH, Zhu X, Privalsky ML, Cheng SY, Stevens RD, Summers SA, et al. Thyroid hormone stimulates hepatic lipid catabolism via activation of autophagy. J Clin Invest 2012; 122:2428-38; PMID:22684107; http://dx.doi.org/10.1172/JCI60580

[13] Pankiv S, Clausen TH, Lamark T, Brech A, Bruun JA, Outzen H, Øvervatn A, Bjørkøy G, Johansen T. p62/SQSTM1 binds directly to Atg8/LC3 to facilitate degradation of ubiquitinated protein aggregates by autophagy. J Biol Chem 2007; 282:24131-45; PMID:17580304; http://dx.doi.org/10.1074/jbc.M702824200

[14] Rajewsky MF, Dauber W, Frankenberg H. Liver carcinogenesis by diethylnitrosamine in the rat. Science 1966; 152:83-5; PMID:5910014; http://dx.doi.org/10.1126/science.152.3718.83

[15] Lozy F, Karantza V. Autophagy and cancer cell metabolism. Semin Cell Dev Biol 2012; 23:395-401; PMID:22281437; http://dx.doi.org/10.1016/j.semcdb.2012.01.005

[16] Qi Y, Chen X, Chan CY, Li D, Yuan C, Yu F, Lin MC, Yew DT, Kung HF, Lai L. Two-dimensional differential gel electrophoresis/analysis of diethylnitrosamine induced rat hepatocellular carcinoma. Int J Cancer 2008; 122:2682-8; PMID:18351647; http://dx.doi.org/10.1002/ijc.23464

[17] Borel F, Kay MA, Mueller C. Recombinant AAV as a platform for translating the therapeutic potential of RNA interference. Mol Ther 2014; 22:692-701; PMID:24352214; http://dx.doi.org/10.1038/mt.2013.285

[18] Sun CP, Wu TH, Chen CC, Wu PY, Shih YM, Tsuneyama K, Tao MH. Studies of efficacy and liver toxicity related to adeno-associated virus-mediated RNA interference. Hum Gene Ther 2013; 24:739-50; PMID:23829557; http://dx.doi.org/10.1089/hum.2012.239

[19] Roessler S, Jia HL, Budhu A, Forgues M, Ye QH, Lee JS, Thorgeirsson SS, Sun Z, Tang ZY, Qin LX, et al. A unique metastasis gene signature enables prediction of tumor relapse in early-stage hepatocellular carcinoma patients. Cancer Res 2010; 70:10202-12; PMID:21159642; http://dx.doi.org/10.1158/0008-5472.CAN-10-2607

[20] Mas VR, Maluf DG, Archer KJ, Yanek K, Kong X, Kulik L, Freise CE, Olthoff KM, Ghobrial RM, McIver PM, et al. Genes involved in viral carcinogenesis and tumor initiation in hepatitis C virus-induced hepatocellular carcinoma. Mol Med 2009; 15:85-94; PMID:19098997; http://dx.doi.org/10.2119/molmed.2008.00110

[21] Pankiv S, Clausen TH, Lamark T, Brech A, Bruun JA, Outzen H, Øvervatn A, Bjørkøy G, Johansen T. p62/SQSTM1 binds directly to Atg8/LC3 to facilitate degradation of ubiquitinated protein aggregates by autophagy. J Biol Chem 2007; 282:24131-45; PMID:17580304; http://dx.doi.org/10.1074/jbc.M702824200

[22] Matsumoto G, Wada K, Okuno M, Kurosawa M, Nukina N. Serine 403 phosphorylation of p62/SQSTM1 regulates selective autophagic clearance of ubiquitinated proteins. Mol Cell 2011; 44:279-89; PMID:22017874; http://dx.doi.org/10.1016/j.molcel.2011.07.039

[23] Lim J, Lachenmayer ML, Wu S, Liu W, Kundu M, Wang R, Komatsu M, Oh YJ, Zhao Y, Yue Z. Proteotoxic stress induces phosphorylation of p62/SQSTM1 by ULK1 to regulate selective autophagic clearance of protein aggregates. PLoS Genet 2015; 11:e1004987; PMID:25723488; http://dx.doi.org/10.1371/journal.pgen.1004987

[24] Connelly S, Mech C. Delivery of adenoviral DNA to mouse liver. Methods Mol Biol 2004; 246:37-52; PMID:14970584

[25] Breyer B, Jiang W, Cheng H, Zhou L, Paul R, Feng T, He TC. Adenoviral vector-mediated gene transfer for human gene therapy. Curr Gene Ther 2001; 1:149-62; PMID:12108952; http://dx.doi.org/10.2174/1566523013348689

[26] Chan IH, Privalsky ML. Thyroid hormone receptor mutants implicated in human hepatocellular carcinoma display an altered target gene repertoire. Oncogene 2009; 28:4162-74; PMID:19749797; http://dx.doi.org/10.1038/onc.2009.265

[27] Gonzalez-Sancho JM, Garcia V, Bonilla F, Munoz A. Thyroid hormone receptors/THR genes in human cancer. Cancer Lett 2003; 192:121-32; PMID:12668276; http://dx.doi.org/10.1016/S0304-3835(02)00614-6

[28] Martinez-Iglesias O, Garcia-Silva S, Tenbaum SP, Regadera J, Larcher F, Paramio JM, Vennström B, Aranda A. Thyroid hormone receptor beta1 acts as a potent suppressor of tumor invasiveness and metastasis. Cancer Res 2009; 69:501-9; PMID:19147563; http://dx.doi.org/10.1158/0008-5472.CAN-08-2198

[29] Chi HC, Chen SL, Liao CJ, Liao CH, Tsai MM, Lin YH, Huang YH, Yeh CT, Wu SM, Tseng YH, et al. Thyroid hormone receptors promote metastasis of human hepatoma cells via regulation of TRAIL. Cell Death Differ 2012; 19:1802-14; PMID:22576662; http://dx.doi.org/10.1038/cdd.2012.58

[30] Yen CC, Huang YH, Liao CY, Liao CJ, Cheng WL, Chen WJ, Lin KH. Mediation of the inhibitory effect of thyroid hormone on proliferation of hepatoma cells by transforming growth factor-β. J Mol Endocrinol 2006; 36:9-21; PMID:16461923; http://dx.doi.org/10.1677/jme.1.01911

[31] Yamada K, Yamamiya I, Utsumi H. In vivo detection of free radicals induced by diethylnitrosamine in rat liver tissue. Free Radic Biol Med 2006; 40:2040-6; PMID:16716904; http://dx.doi.org/10.1016/j.freeradbiomed.2006.01.031

[32] Bechtel W, Bauer G. Modulation of intercellular ROS signaling of human tumor cells. Anticancer Res 2009; 29:4559-70; PMID:20032404

[33] Calvisi DF, Ladu S, Gorden A, Farina M, Conner EA, Lee JS, Factor VM, Thorgeirsson SS. Ubiquitous activation of Ras and Jak/Stat pathways in human HCC. Gastroenterology 2006; 130:1117-28; PMID:16618406; http://dx.doi.org/10.1053/j.gastro.2006.01.006

[34] Scherz-Shouval R, Elazar Z. Regulation of autophagy by ROS: physiology and pathology. Trends Biochem Sci 2011; 36:30-8; PMID:20728362; http://dx.doi.org/10.1016/j.tibs.2010.07.007

[35] Limoli CL, Giedzinski E, Morgan WF, Swarts SG, Jones GD, Hyun W. Persistent oxidative stress in chromosomally unstable cells. Cancer Res 2003; 63:3107-11; PMID:12810636

[36] Klionsky DJ, Abdelmohsen K, Abe A, Abedin MJ, Abeliovich H, Acevedo Arozena A, Adachi H, Adams CM, Adams PD, Adeli K, et al. Guidelines for the use and interpretation of assays for monitoring autophagy (3rd edition). Autophagy 2016; 12:1-222; PMID:26799652; http://dx.doi.org/10.1080/15548627.2015.1100356